contribution of the bremsstrahlung occurs at low energies where the scatter of our data is large, so that a modest uncertainty in the value of k does not appreciably increase the uncertainty in our final results.

[6]E. H. S. Burhop and W. N. Assad, Adv. At. Mol. Phys. 8, 163 (1972).

[7]C. J. Sparks, Jr., Phys. Rev. Lett. 33, 262 (1974).

[8]The partial polarization of our incident beam should lead to a small increase in intensity (by a factor of order $\frac{4}{3}$) over that calculated for an unpolarized beam.

[9]Y. B. Bannett and I. Freund, Phys. Rev. Lett. 34, 372(C) (1975).

Localization of Conduction Electrons by Fe, Co, and Ni in $1T$-TaS_2 and $1T$-$TaSe_2$

F. J. Di Salvo, J. A. Wilson, and J. V. Waszczak
Bell Laboratories, Murray Hill, New Jersey 07974

(Received 12 December 1975)

$1T$-$M_x Ta_{1-x} S_2$ or $1T$-$M_x Ta_{1-x} Se_2$ with M= Fe, Co, or Ni shows large increases in resistivity at low temperatures when $\frac{1}{3} > x \geq x_c$ ($x_c \approx 0.02$ for the disulfides, and 0.15 for the diselenides). We suggest that this increase is due to Anderson localization of the conduction electrons by the random potential of M. However, in contrast to the usual impurity state in metals, the presence of a charge-density wave makes this potential temperature dependent and long ranged.

Following the discovery of the charge-density-wave (CDW) state in layered compounds,[1] we undertook extensive studies of the effects of doping on the CDW.[2] Recently, we discovered that large amounts of Fe, Co, or Ni could be randomly substituted for Ta in $1T$-TaS_2 and $1T$-$TaSe_2$.[3] Beyond a critical doping level, the random potential of the $3d$ cations causes the resistivity to increase rapidly with decreasing temperature. We speculate that a modification of the Anderson transition[4] occurs, a modification due to the CDW, to the $3d$ cations, and to their mutual interaction.

X-ray diffraction of the powder products shows that the maximum substitution possible in $1T$-TaS_2 and $1T$-$TaSe_2$ is $\frac{1}{3}$ for Fe and Co, but only ≈ 0.2 for Ni. In the case of Ni, for $x \gtrsim 0.2$, a complex set of superlattice lines appear, which we are presently unable to index. The actual ratio of cation concentration in single crystals was determined by x-ray fluorescence.

A measurement of the magnetic susceptibility (χ) by the Faraday method from 4.2 to 850°K (on powders at $x = 0.1$) shows the dopant M to be primarily divalent. For $T \gtrsim 2\Theta$, χ fits the expression

$$\chi = \chi_0 + C/(T + \Theta), \quad (1)$$

where

$$C = N\mu_{\mathrm{eff}}^2/3k.$$

χ_0 is expected to be somewhat temperature dependent because of the Pauli contribution, as in $1T$-$Ti_x Ta_{1-x} S_2$.[2] The antiferromagnetic Weiss constant, Θ, increases with increasing x. Table I summarizes the data for the sulfides. Similar results are found for the selenides, except that Co loses its moment. The Fe-doped compounds show a change from low to high spin with increasing T. For low x, Mössbauer measurements[5] show that Fe remains divalent through this change.

The above leads us to formulate these compounds as $1T$-$(3d^{2+})_x (Ta^{5+})_{2x} (Ta^{4+})_{1-3x} X_2$ (at least at low x), where X = S or Se. The disproportionation of the Ta valence occurs readily. X-ray photoelectron spectroscopy measurements show that at 300°K the CDW amplitude (in the conduction-electron density) for undoped $1T$-TaS_2 is ≈ 1 electron per atom[6] and thus some Ta with an effective valence near 5 must exist even there (CDW onset temperature $T_0 = 600$°K[1,2]).

200-kV transmission electron diffraction patterns for $x \leq 0.10$ are similar to those of $1T$-

TABLE I. The effective magnetic moments (in units of the Bohr magneton, μ_B), and the antiferromagnetic Weiss constants, Θ, for $x = 0.10$. The former values show the $3d$ cations to the be close to divalent.

M	μ_{eff}	Θ (K)	μ_{eff} for ideal 2+ $g=2$
Ni	2.55	20	2.83
Co	1.48	5	1.73
Fe	0 ($T < 200$)	...	Low spin

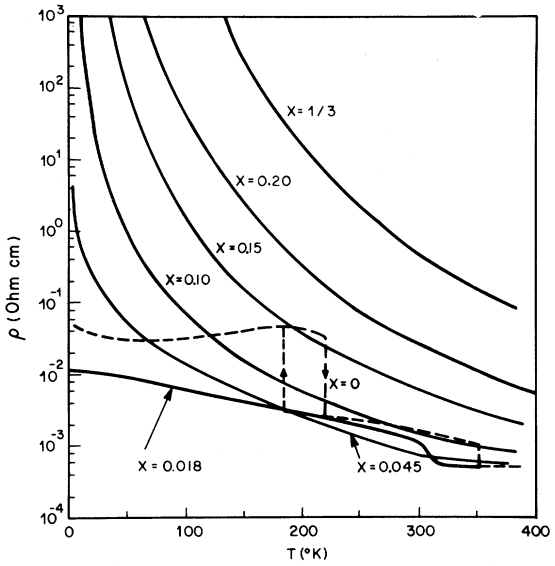

FIG. 1. The resistivity of $1T$-$Fe_xTa_{1-x}S_2$ layered compounds (current parallel to the layers) shows large increases at low temperatures when $x \gtrsim 0.02$ ($=x_c$), smoothly growing out of the CDW state of $1T$-TaS_2.

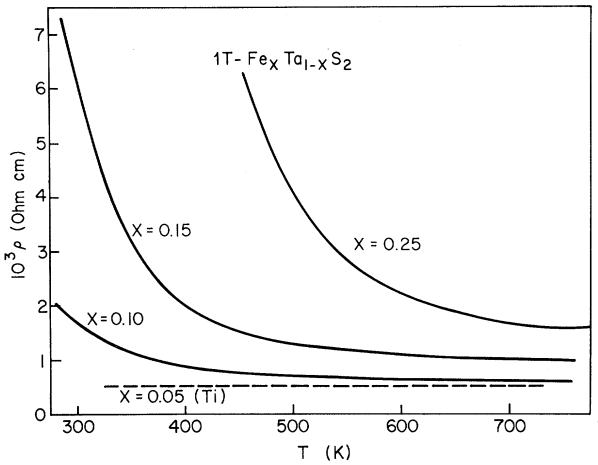

FIG. 2. Above ≈ 600°K, the resistivity of $1T$-Fe_x-$Ta_{1-x}S_2$ compounds for $x \leq 0.25$ is only slightly temperature dependent.

$Ta_{1-x}Ti_xS_2$ [1] and show the presence of an incommensurate CDW. Sharp satellite spots separated from the main Bragg peaks by $\vec{q}_0$ are seen, in addition to circular diffuse-scattering rings. For $x \geq 0.15$ the satellite spots are weaker and broader and become difficult to separate from the diffuse-scattering rings, indicating a very short coherence length for the CDW and its concurrent lattice distortions. $\vec{q}_0$ decreases with increasing x; the initial decrease, $d(q_0'/a^*)/dx$, is 0.32 for Fe, 0.26 for Co, and 0.40 for Ni. (q_0' is the basal-plane projection of $\vec{q}_0$.) These numbers are approximately twice the value found in $1T$-Ta_{1-x}-Ti_xS_2 (0.16). A full account and interpretation of these studies will be published separately.

The electrical resistivities (ρ) for single-crystal $1T$-$Fe_xTa_{1-x}S_2$ are shown in Fig. 1. The dashed curve for pure $1T$-TaS_2 shows two first-order transitions toward the commensurate CDW state at $T_d' = 352$°K and $T_d = 200$°K.[1,2,7] These transitions are eliminated for $x \geq 0.05$ because of the disorder, as is found with other cation dopants.[2]

Despite the dramatic low-temperature behavior, at high temperature ρ is only slightly temperature dependent. The value is somewhat above 5×10^{-4} Ω cm obtained for $1T$-TaS_2 or $1T$-$Ta_{0.95}$-$Ti_{0.05}S_2$ (Fig. 2). An increased ρ at high temperatures with increasing x is consistent with the expected decrease of Ta^{4+} concentration. The values of resistivity at high T indicate that most of the carriers contribute to the conductivity, but the impurity scattering is large, as in many transition-metal alloys.[8]

The same general resistivity behavior is also seen in $1T$-$Fe_xTa_{1-x}Se_2$ (Fig. 3). Again the transition to the commensurate CDW state ($T_d = 473$°K; CDW onset at $T_0 \approx 600$°K) is removed for $x > 0.05$, but now more Fe is required ($x_c \approx 0.15$) than in the sulfide ($x_c \approx 0.02$) to produce an increasing ρ at low T.

Also the same resistive behavior occurs when the dopant is Co or Ni (see Fig. 4 for 10% Fe, Co, and Ni doping in $1T$-TaS_2). The low-temperature increase is dramatic when compared with quadrivalent Nb or V doping.[2]

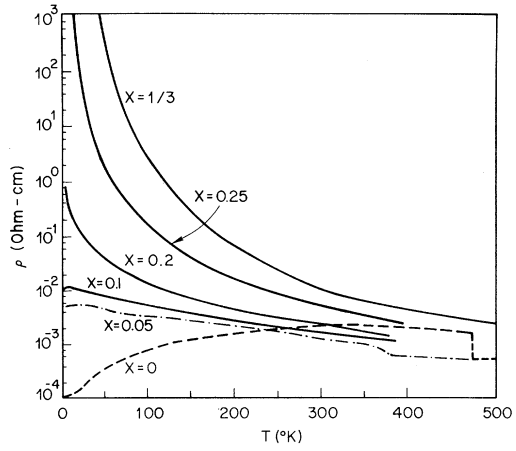

FIG. 3. The resistivity of $1T$-$Fe_xTa_{1-x}Se_2$ parallel to the layers. Larger doping than in $1T$-TaS_2 is necessary to produce an increasing ρ at low T ($x_c \sim 0.15$).

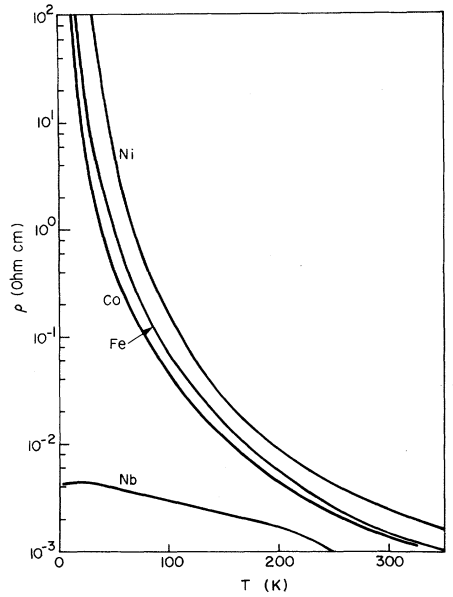

FIG. 4. A comparison of the resistivities of $M_{0.1}Ta_{0.9}S_2$, M= Fe, Co, Ni, and Nb. When compared with $1T$-$Nb_{0.1}Ta_{0.9}S_2$, the low-temperature increase for the $3d$-doped samples is dramatic.

ρ for $T \leq 100$°K is fitted by the expression

$$\rho(T) = \rho_0 (T_0/T)^{a(x-x_c)}, \quad (2)$$

when $x > x_c$ (see Fig. 5). For example, in $1T$-$Fe_xTa_{1-x}S_2$ we find $\rho_0 \sim 0.16\ \Omega$ cm, $T_0 \sim 385$°K, and $a \sim 37$ ($x \leq 0.25$). This is an entirely empirical fit, and presently uninvestigated theoretically. In many disordered materials $\rho(T)$ follows the theoretically expected form[9]

$$\rho(T) \propto \exp(T_0/T)^n, \quad 1 > n > \tfrac{1}{4}. \quad (3)$$

However, data for the present materials are not fitted by Eq. (3) over this range of n (Fig. 5).

A large increase in ρ at low T has also been observed in nominal $1T$-$Fe_{0.05}Ta_{0.95}S_2$ by Fleming and Coleman.[10] However, $\rho(T)$ for our samples continues to rise when $T < 4.2$°K, in contrast to the leveling off that they report.

The data are consistent with the general ideas of loss of conduction-electron mobility due to disorder[4] (Anderson transition). It is clear that the magnetic state of the $3d$ cation is not correlated with the increasing $\rho(T)$ at low T, since the moments of the Fe, Co, and Ni are so different (indeed for Fe at low T, $\mu_{\text{eff}} = 0$). The model predicts *at zero temperature* that as the random potential, V_0, is increased relative to the bandwidth, B, the conductivity decreases to a minimum value $\sigma_{\min}$ at $V_0/B \sim 1$, beyond which $\sigma = 0$.

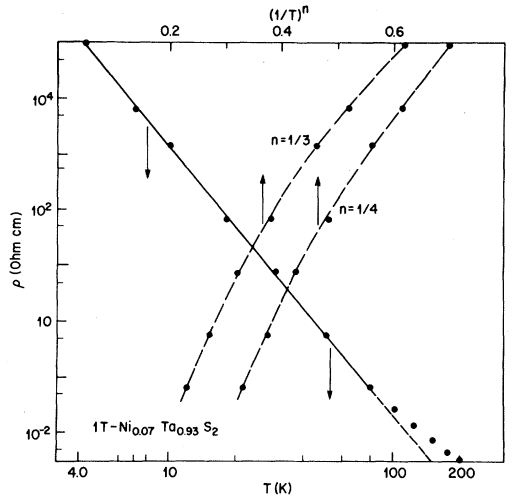

FIG. 5. $\ln\rho$ versus $\ln T$ for $1T$-$Ni_{0.07}Ta_{0.93}S_2$ shows the straight-line fit by Eq. (2). Also shown is the inadequacy of Eq. (3) in fitting the data for $n = \frac{1}{4}$ and $\frac{1}{3}$ [$\ln\rho$ versus $(1/T)^n$].

An increase in the random potential is produced in our samples by increasing x. σ remains finite *at* $T = 0$ for $x \leq x_c$, but extrapolates to zero for $x > x_c$. We find that $\sigma_{\min}$ is $\approx 40\ \Omega^{-1}$ cm^{-1}, the same order of magnitude expected from the theory.[4]

However, these materials differ from those to which the theory is usually applied in several important ways. With a CDW present below $T_0 \sim 600$°K, both the conduction-electron density and the magnitude of the random potential are now temperature dependent. The CDW produces gaps at the Fermi surface, which steadily reduce the carrier density (increasing ρ in the pure $1T$ compounds, as in Figs. 1 and 3). Secondly, the disturbance introduced by each M is amplified over that expected in a normal metal by a local temperature-dependent CDW "cloud."[11] *It seems likely that without the CDW, the present strong effects would not be observed.* Cation disorder in normal metallic alloys does not produce such dramatic effects. These differences, along with the very high density of localizing centers, are most likely responsible for the deviation of the low-temperature $\rho(T)$ from that obtained in the usual Anderson-type localization.

We would like to acknowledge useful discussions with and suggestions by M. Eibschutz, D. E. Moncton, T. M. Rice, and G. K. Wertheim. We thank G. W. Hull for performing some of the low-temperature ρ measurements and S. Mahajan for continued collaboration in electron microscopy.

[1]J. A. Wilson, F. J. Di Salvo, and S. Mahajan, Adv. Phys. 24, 117 (1975).
[2]F. J. Di Salvo, J. A. Wilson, B. G. Bagley, and J. V. Waszczak, Phys. Rev. B 12, 2220 (1975).
[3]F. J. Di Salvo, M. Eibschutz, J. A. Wilson, and J. V. Waszczak, Bull. Am. Phys. Soc. 20, 290 (1975).
[4]N. F. Mott, M. Pepper, S. Pollitt, R. H. Wallis, and C. J. Adkins, Proc. Roy. Soc. London, Ser. A 345, 169 (1975).
[5]M. Eibschutz and F. J. Di Salvo, to be published.
[6]G. K. Wertheim, F. J. Di Salvo, and S. Chiang, Phys. Lett. 54A, 304 (1975).
[7]A. H. Thompson, F. R. Gamble, and J. F. Revelli, Solid State Commun. 9, 981 (1971).
[8]G. T. Meaden, *Electrical Resistance of Metals* (Plenum, New York, 1965).
[9]E. M. Hamilton, Philos. Mag. 26, 1043 (1972).
[10]R. M. Fleming and R. V. Coleman, Phys. Rev. Lett. 34, 1502 (1975).
[11]W. L. McMillan, Phys. Rev. B 12, 1187 (1975).

Polarization Echoes and Long-Time Storage in Piezoelectric Powders

R. L. Melcher and N. S. Shiren
IBM Thomas J. Watson Research Center, Yorktown Heights, New York 10598
(Received 8 January 1976)

Two- and three-pulse polarization echoes are detected in powders of mechanically resonant particles of piezoelectric materials. Under some conditions the decay time of the three-pulse echo can be of order one day or longer. A model for the echo formation and long decay time based upon the torque exerted on an oscillating dipole by an applied rf field is described.

The linear absorption and radiation of radio-frequency energy by electromechanical oscillations of piezoelectric particles has been known for some time.[1] Similar effects have been observed in particles of magnetoelastic materials.[2] Subsequently polarization echoes have been reported in magnetoelastic[3] and piezoelectric[4] powders. In polarization-echo experiments, as is also the case in spin echoes, rf pulses are applied to the powder samples at times $t=0$, τ, and T. The two-pulse echo, e_2, is radiated by the sample at $t=2\tau$ and the three-pulse echo, e_3 is radiated at $t=T+\tau$. The relaxation times T_2 and T_1 are defined by $e_2 \propto \exp(-2\tau/T_2)$ and $e_3 \propto \exp(-2\tau/T_2 - T/T_1)$. In piezoelectric powders T_2 and T_1 are typically 10^{-3} sec or less. However, recent experiments[5-8] have shown that the relaxation time T_1 can exceed days in some cases. Relaxation times of this magnitude must be attributed to some static or stored polarization property of the powder sample and cannot be associated with any dynamic behavior of the system.

In this Letter we report new experimental and theoretical results on the polarization-echo storage phenomenon in powders of mechanically resonant particles of piezoelectric materials. We have detected the storage effect in several piezoelectric materials at radio frequency (20–200 MHz) and in one material, ZnO, at X-band microwave frequencies (9 GHz). We propose a model to explain the mechanism of echo formation and the origin of the decay time, T_1, of the three-pulse or "stimulated" echo.

In our experiments the amplitude of the rf electric field pulses applied to the powder sample were of order 5×10^3 V/cm and the pulse widths were of order 10^{-6} sec. In strongly piezoelectric materials the echo signals are quite intense. For example in a 1-cm^3 sample of $LiNbO_3$ powder, peak radiated echo powers of order 10^{-1} W were detected on application of peak pulse powers of order 10^3 W. Application of a single rf pulse to a mechanically resonant sample causes the individual particles to oscillate or "ring" at their natural frequencies. This ringing is detected after each pulse as a somewhat irregular signal which decays approximately exponentially. This decay as well as the T_2 from the echo decay was found to be dependent upon particle size, frequency, temperature, particle packing density, and particle surface finish. In addition, two-pulse echoes were detected in powders of every piezoelectric material we studied, including natural and hydrothermally grown quartz, sand, CdS, CdTe, ZnO, ZnSe, GaAs, $BaTiO_3$, $LiNbO_3$, K_x-$Li_{1-x}NbO_3$, $LiTa_{0.8}Nb_{0.2}O_3$, Li_2GeO_3, $Gd_2(MoO_4)_3$, SbSI, Se, PLZT (lead-based, lanthanum-doped zirconate titanate) ceramic, $RbAg_4I_5$, and triglycine sulfate. Other workers have reported on additional materials.[4-7] In the absence of con-